Biomagnetics

Harmonic Simulation Study of Simultaneous Nanoparticle Size and Viscosity Differentiation

Carolyn Shasha[1], Eric Teeman[2], and Kannan M. Krishnan[1,2]

[1] Department of Physics, University of Washington, Seattle, WA 98195, USA
[2] Department of Materials Science and Engineering, University of Washington, Seattle, WA 98195, USA

Received 30 Jun 2017, revised 15 Aug 2017, accepted 7 Sep 2017, published 18 Sep 2017, current version 11 Oct 2017.

Abstract—The signal harmonics of magnetic nanoparticles in solution under an ac magnetic field are highly sensitive to their physical properties and the surrounding environment. Here, we use Monte Carlo simulations of coupled stochastic Langevin equations to demonstrate a possible technique that can simultaneously characterize different particle sizes and viscous environments. When combined with a constant bias field, the relative amplitudes of the harmonics change significantly, and are shown to be uniquely sensitive to changes in particle size and viscosity. Spectroscopic experiments verify the size-dependent harmonic behavior. With this technique, particles with sizes differing by only ∼1–2 nm in diameter can theoretically be identified, while separately quantifying changes in viscosity. This concurrent characterization could be implemented in magnetic particle imaging to create a colorized image.

Index Terms—Biomagnetics, magnetic nanoparticles, harmonic analysis, monte carlo simulations, particle sizes, magnetic relaxation.

I. INTRODUCTION

Magnetic particle imaging (MPI) is an emerging medical platform that measures the response of magnetic nanoparticles (MNPs) to an ac magnetic field, which can be processed to create an image [Gleich 2005, Weizenecker 2009, Krishnan 2010]. Recently, there have been explorations into the possibility of creating multicolor images using MPI by separating the signal from MNPs of different sizes or in varying chemical or viscous environments, which could substantially increase the translational scope of MPI [Rahmer 2015]. Magnetic spectroscopy of nanoparticle Brownian motion (MSB) is the technique of using the signal harmonics to determine the microscopic environment of nanoparticles [Weaver 2008]. The harmonics, obtained by taking a simple Fourier transform of the magnetic response signal, provide a strong potential basis for multicolor imaging because of their high sensitivity to particle conditions.

Several specific approaches to multicolor spectroscopy have been proposed [Rauwerdink 2010, Hensley 2015, Wu 2015]; however, they all have significant limitations. Previous techniques have so far only demonstrated potential for differentiation between particles of substantially different sizes (differences in particle diameters of ∼10–15 nm). However, for a strong MPI signal, particles must be restricted to a relatively narrow range of sizes tailored to the applied frequency; otherwise signal will be dramatically lowered [Ferguson 2011]. Consequently, realistic multicolor imaging requires differentiation between particles whose diameters are only a few nanometers apart. Furthermore, the MNP spectroscopic response is strongly dependent on the surrounding environment, particularly viscosity (for Brownian particles), as has been shown with MSB [Rauwerdink 2011]. Previous proposed techniques for size differentiation require that the particles be in environments with identical viscosities, which may not be the case in practical biological applications. Information about the viscosity of MNP environment itself is desirable, as it can provide information about nanoparticle binding or blood viscosity as an indication of disease [Lee 2012].

Here, we demonstrate a technique for separately differentiating between both MNP size and viscosity, by varying the magnitude of an additional constant magnetic field in the direction of the alternating field and recording the harmonics. The application of a bias field has been proposed previously as a method to increase overall response signal [Weaver 2008], and can be easily implemented in current MPI systems with a simple offset of one of the gradient fields [Krishnan 2016]. The MNP nonlinear response to magnetic fields used for MPI is complex, and equations describing the dynamics cannot be solved in closed form. Consequently, alternative methods, such as stochastic simulations, are required in order to obtain accurate behavior of the harmonics under realistic biosensing conditions. In this paper, we use Monte Carlo simulations of coupled stochastic Langevin equations to show that the addition of a bias field results in size- and viscosity-dependent maxima in the third harmonic. We verify the size-dependent behavior experimentally, and use simulations to predict the response under realistic MPI conditions. The odd harmonic phase angles have been previously shown to exhibit size-dependent behavior [Rauwerdink 2010]; we confirm this, and predict the specific phase angle response to small changes in size and viscosity, which can be used as additional independent parameters for particle identification.

II. THEORY

A. Relaxation Timescales

In MPI, nanoparticles rotate under the influence of an external oscillating field, generating a measureable signal [Krishnan 2016]. The resulting particle dynamics are typically discussed in terms of timescales of nanoparticle rotations, particularly the *equilibrium* relaxation

Corresponding author: Carolyn Shasha (e-mail: cshasha@uw.edu).
This paper has supplementary downloadable material available at http://ieeexplore.ieee.org.
Digital Object Identifier 10.1109/LMAG.2017.2754238

time. MNPs can relax via two mechanisms: Brownian and Néel relaxation. The characteristic Brownian relaxation time, which describes the physical rotation of the particle, is [Rosensweig 2002]

$$\tau_B = \frac{3V_h\eta}{k_BT} \tag{1}$$

where V_h is the hydrodynamic volume of the particle, η is the viscosity of the surrounding medium, k_B is Boltzmann's constant, and T is the temperature. In addition to Brownian relaxation, the magnetic moment of the nanoparticle can flip internally. This process is called Néel relaxation, and is characterized by the relaxation time [Coffey 2012]

$$\tau_N = \frac{\sqrt{\pi}}{2}\tau_0\frac{\exp(\sigma)}{\sqrt{\sigma}} \tag{2}$$

where τ_0, the attempt time, is a constant on the order of 10^{-10} [Rosensweig 2002], and $\sigma = KV_C/k_BT$, where V_c is the particle core volume, and K is the uniaxial anisotropy constant. MNPs will typically relax via a combination of these two mechanisms [Shah 2015]. The effective relaxation time will determine the overall phase lag between the driving field and the magnetization response, which indicates that the response will be dependent on the same properties as the relaxation timescales, such as size and viscosity.

B. Linear Dynamics

Under an oscillating field, the average magnetization of a collection of nanoparticles can be plotted against the applied field. In the simplest interpretation, if particles are assumed to be isotropic, noninteracting, and identical, the magnetization is proportional to the Langevin function [Krishnan 2016]

$$L(\xi) = \frac{M(\xi)}{M_S} = \coth\xi - \frac{1}{\xi} \tag{3}$$

where $\xi = V_cM_SH/k_BT$, M_S is the saturation magnetization, and H is the applied magnetic field. With the addition of a constant bias field, the total applied field is

$$H = H_0\cos(\omega t) + H_{\text{bias}} \tag{4}$$

where ω and H_0 are the frequency and amplitude of the ac field. Inserting this into the Langevin function, we can perform a Fourier expansion on the magnetization. Fig. 1(a) shows that variation of the magnitude of the bias field results in distinct peaks in the harmonics. Importantly, the location and shape of these peaks are size dependent, as shown in Fig. 1(b).

C. Nonlinear Dynamics

The qualitative behavior seen in Fig. 1 suggests that measurements of the third harmonic under an offset field can be employed for particle size differentiation; however, to verify applicability for MPI, more sophisticated models are necessary. The Langevin function applies only when equilibrium is a valid approximation, e.g., in the limit $\frac{1}{f} \gg \tau$. Consequently, for MPI, which employs ac field frequencies on the order of tens of kilohertz and particles with a core diameter >20 nm, the Langevin function is not a good approximation. To study the nonlinear dynamics of nanoparticles under realistic MPI conditions, we use Monte Carlo simulations, solving combined stochastic differential equations described in detail in Coffey [1993]. The particles are able to rotate via both Brownian and Néel mechanisms.

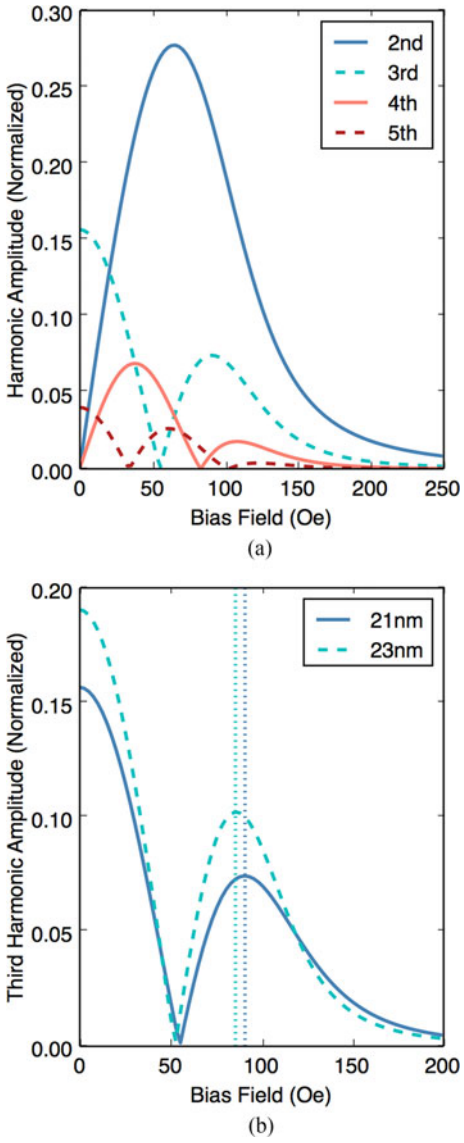

Fig. 1. Harmonic signals produced by identical nanoparticles according to the Langevin function with an ac field of 100 Oe and frequency 1 kHz, normalized to the maximum amplitude of the first harmonic. (a) Second, third, fourth, and fifth harmonics of a 21 nm (diameter) particle. Dashed lines indicate odd harmonics, and solid lines indicate even harmonics. (b) The amplitude of the third harmonic for two particle sizes, 21 and 23 nm. Vertical dotted lines indicate the location of the second maxima, which is different for each size.

The internal magnetization direction $\mathbf{m}$ will rotate according to the Landau–Lifshitz–Gilbert equation, which will be coupled to the differential equation describing the general torque exerted on the easy axis $\mathbf{n}$

$$\frac{d\mathbf{m}}{dt} = \frac{\gamma}{1+\alpha^2}(\mathbf{H} + \alpha\mathbf{m}\times\mathbf{H})\times\mathbf{m} \tag{5}$$

$$\frac{d\mathbf{n}}{dt} = \frac{\theta}{6\eta V_h}\times\mathbf{n} \tag{6}$$

where γ is the electron gyromagnetic ratio and α is the damping coefficient. The effective magnetic field $\mathbf{H}$ and the effective torque θ are determined from the total particle energy

$$U = -\mu\mathbf{m}\cdot\mathbf{H}_{\text{app}} - KV_c(\mathbf{m}\cdot\mathbf{n})^2. \tag{7}$$

Here, μ represents the magnitude of the particle's magnetic moment equal to $V_c M_S$. The first term represents the Zeeman interaction with the applied field $\mathbf{H}_{\text{app}}$. The second term is the energy contribution from the effective particle anisotropy. We assume that the particles will sufficiently disperse, so that dipolar interactions can be ignored. The effective magnetic field and torque can then be found by taking derivatives of the energy and adding thermal fluctuations

$$\mathbf{H} = \frac{1}{\mu}\frac{\partial U}{\partial \mathbf{m}} + \mathbf{H}_{\text{th}} = \mathbf{H}_{\text{app}} + \frac{2KV_c}{\mu}(\mathbf{m}\cdot\mathbf{n})\,\mathbf{n} + \mathbf{H}_{\text{th}} \tag{8}$$

$$\theta = \frac{\partial U}{\partial \mathbf{n}} \times \mathbf{n} + \theta_{\text{th}} = -2KV_c\,(\mathbf{m}\cdot\mathbf{n})\,(\mathbf{m}\times\mathbf{n}) + \theta_{\text{th}}. \tag{9}$$

The thermal fluctuation field and torque are each assumed to be a Gaussian stochastic process with mean zero ($\mathbf{H}^i_{\text{th}}(t) = 0$ and $\theta^i_{\text{th}}(t) = 0$) and correlations $\mathbf{H}^i_{\text{th}}(t)\mathbf{H}^j_{\text{th}}(t') = \frac{2k_BT}{\gamma\mu}\frac{1+\alpha^2}{\alpha}\delta_{ij}\delta(t-t')$ and $\theta^i_{\text{th}}(t)\theta^j_{\text{th}}(t') = 12k_BT\eta V_h\delta_{ij}\delta(t-t')$. To integrate these equations, we use the Stratanovitch–Heun method, following others [Shah 2014, Reeves 2015, Shah 2015], which can properly account for the stochastic terms in the white-noise limit [Kloeden 1992], shown in further detail in the supplemental material.

III. MATERIALS AND METHODS

A. Sample Preparation and Measurement

Three sizes of iron oxide nanoparticles were synthesized in our laboratory following procedures described in detail elsewhere [Hufschmid 2015, Kemp 2016]. The average particle sizes and distribution parameters were measured with TEM and obtained from fitting to a log-normal size distribution. The three samples had average diameters (size distribution parameters) of 21 nm (0.05), 23.8 nm (0.05), and 25.2 nm (0.09). Particles were dispersed in water mixed with 1% low-melting point agarose to reduce interactions between particles, and subsequently lyophilized, immobilizing the particles. Magnetic measurements were taken at 300 K with a Quantum Design Physical Property Measurement System, which is able to measure the complex harmonics of the magnetization response.

B. Simulation Parameters

Simulations were performed at 300 K with uniaxial anisotropy constant $K = 3.5 \pm 0.5$ kJ/m^3 [Ludwig 2014] and saturation magnetization $M_s = 420$ kA/m. The same size distribution parameters that were determined by TEM were used, with a default value of 0.05. When running the simulations, the easy axis and magnetic moment direction of each particle were initialized separately to a random orientation. The particles were then allowed to thermalize for a number of time steps (one-fifth of the total time steps used for the main simulation). About 4000 particles were simulated at a time, with their magnetization averaged over 10–50 independent iterations (more iterations were required for simulations at lower ac field amplitude, for better resolution).

IV. RESULTS AND DISCUSSION

We first verify experimentally the behavior shown in Fig. 1. Under a sweep of an applied bias field, a peak in the third harmonic is visible, the location of which changes based on particle size, seen in Fig. 2. The third and fifth harmonic phase angles, shown in the inset, are clearly distinct. Since the particles are immobilized, viscosity effects are not a factor and Néel relaxation will dominate. Due to instrument limitations, a lower amplitude field of 13 Oe was applied, with a frequency 10 kHz. Simulations, performed with a 13 Oe/10 kHz field, match the data and indicate a size-dependent maximum in the third harmonic as well. Qualitative differences between Fig. 2 and the Langevin function predictions are primarily due to the difference in ac field amplitude (100 Oe in Fig. 1 and 13 Oe in Fig. 2).

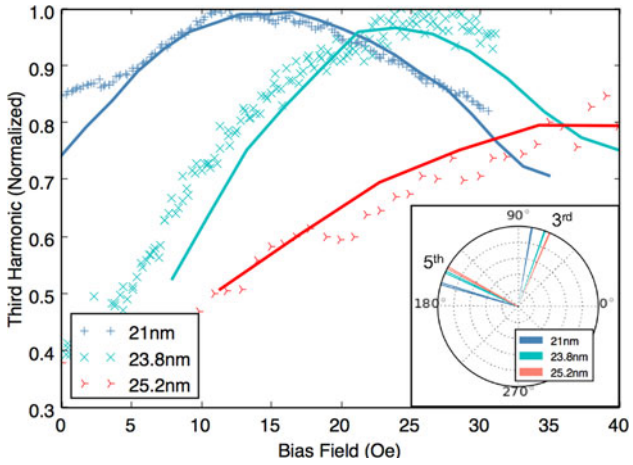

Fig. 2. (Markers) Experimental data and (solid lines) simulations of the third harmonic of particles of three sizes (21 nm, 23.8 nm, 25.2 nm) from an ac field with amplitude 13 Oe and frequency 10 kHz. Inset: Experimental data of (solid bars) the third and (open bars) fifth harmonic phase angles of the same three samples. Simulations of the phase angle follow the same trend as the measured phase angle, but are omitted for clarity.

Under realistic biosensing conditions, free particles will also be able to physically rotate in fluid. To understand this complex behavior, we simulate particles with identical physical parameters, but under conditions more realistic for MPI, with an ac field of 100 Oe and frequency of 25 kHz. Particles are allowed to physically rotate, and viscosity is set to that of water, 1 cp. The location and height of the second maximum in the third harmonic still varies significantly with particle size, as seen in Fig. 3. These simulations are repeated for 11 total particle sizes, and the location of the middle peak is shown to decrease with diameter in the inset of Fig. 3. The third and fifth phase angles at zero bias field are also simulated, and are plotted for the same 11 sizes in Fig. 4. The phase angles monotonically decrease with increasing size. The peak of the third harmonic plus the third and fifth phase angles provide three independent measurements that can be used to concurrently identify multiple particle sizes, assuming constant viscosity. Although only the third harmonic is shown here, peaks in the amplitudes of the second, fourth, fifth, and even higher harmonics (dependent on total signal and resolution) could be used as additional parameters. While the even harmonics typically do not contribute to MPI signal, application of a bias field introduces nonzero even harmonics.

Harmonic amplitude and phase angle vary substantially with viscosity as well. To investigate this effect, we perform simulations with varying viscosity at fixed particle size, shown in Fig. 5. The location of the second maximum in the third harmonic shifts with changing viscosity, similar to changing particle size. However, when a bias field greater than ~150 Oe is applied, the third harmonic amplitude exhibits distinct viscosity-dependent behavior that is not seen with small size

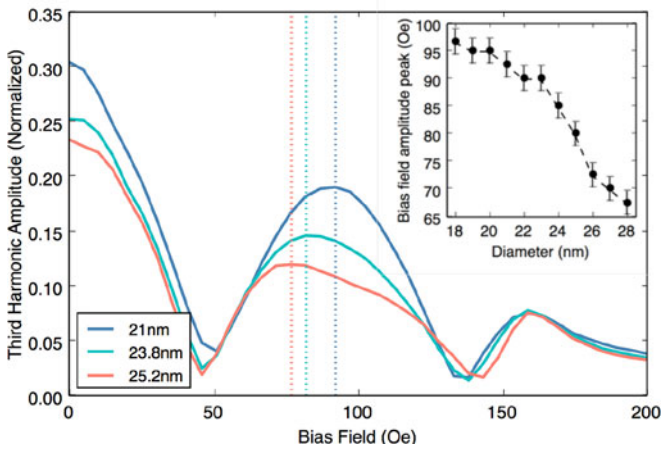

Fig. 3. Monte Carlo simulations of the third harmonic, normalized to the maximum of the first harmonic, for three particle sizes (21 nm, 23.8 nm, 25.2 nm) under an ac field with amplitude 100 Oe and frequency 25 kHz. Vertical dotted lines indicate the location of the second maxima. Inset: Bias field magnitude corresponding to the location of the second maximum as a function of particle diameter.

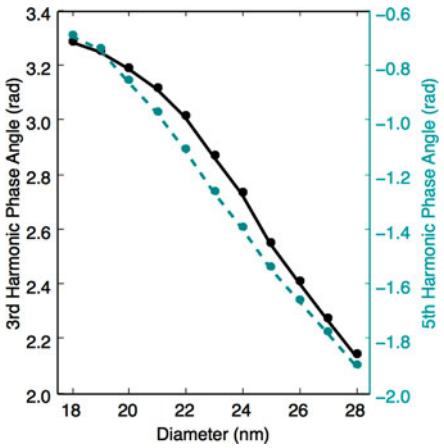

Fig 4. Monte Carlo simulations of (black, solid) the third and (blue, dashed) fifth harmonic phase angles under an ac field with amplitude 100 Oe and frequency 25 kHz, at zero bias field, plotted as a function of particle diameter.

variation. As the bias field is increased, the third harmonic amplitude decreases to a second minimum after the peak, but then rises again and levels out at a nonzero value. The amplitude of the third harmonic is normalized to the maximum of the first harmonic, to remove the influence of total sample mass. When the particles are completely immobilized, no additional maximum is seen, and the third harmonic reduces to zero at high bias fields. This unique behavior can be used to determine the viscosity separately from particle size. From the "tail height" (the magnitude of the third harmonic at high bias fields, here chosen to be 250 Oe), the viscosity and expected peak location can be determined (shown in the inset of Fig. 5). Differences between the expected peak location and measured peak location are a result of difference in particle size, which is then determined from the relationship between size and peak location (i.e., from the plot in the inset of Fig. 3).

The third and fifth harmonic phase angles at zero bias field again act as additional independent parameters. They show distinctly different

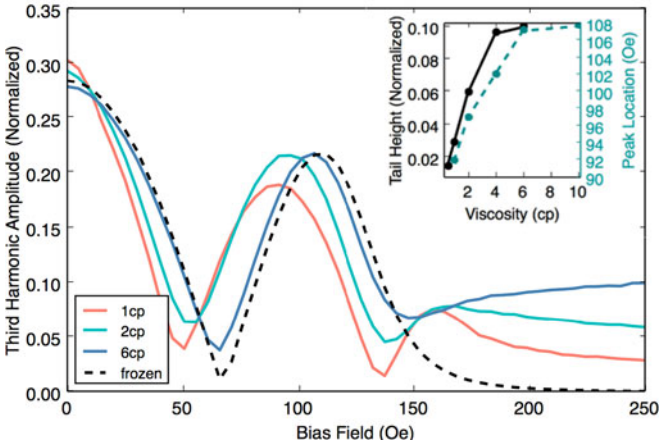

Fig. 5. Monte Carlo simulations of the third harmonic, normalized to the maximum of the first harmonic, for three viscosities (1cp, 2cp, 6cp, solid lines), plus immobilized particles (black dashed line) under an ac field with 100 Oe and frequency 25 kHz. Inset: Third harmonic amplitude at a bias field of 250 Oe ("tail height"), versus (black line) viscosity, and (blue dashed line) bias field magnitude corresponding to the location of the second maximum in the third harmonic versus particle diameter.

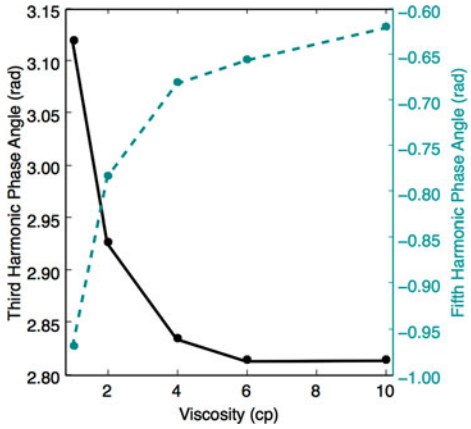

Fig. 6. Monte Carlo simulations of (black, solid) the third and (blue, dashed) fifth harmonic phase angles under an ac field with amplitude 100 Oe and frequency 25 kHz, at zero bias field, plotted as a function of viscosity.

behavior under increasing viscosity than with increasing particle diameter (see Fig. 6). With a simple calibration measurement of separate nanoparticles, both in a known viscosity and in an immobilized state, multiple nanoparticle sizes and viscosities could be identified and quantified. The number of independent parameters, which determines the number of different sizes and types that can be distinguished, is dependent on the higher harmonics' signal strength.

V. CONCLUSION

With the above theoretical results, we demonstrate a method for separately differentiating between particle size and viscosity from harmonics information, improving upon previous proposed techniques. We demonstrate high sensitivity to both particle diameter and viscosity, showing that particles that differ by ∼1–2 nm in diameter can be separately resolved, indicating possible implementation in MPI. Experimental work to confirm these predictions, in the context of developing a method for introducing "color" in magnetic particle imaging, is under progress.

ACKNOWLEDGMENT

This work was supported by the National Science Foundation Graduate Research Fellowship under Grant DGE-1256082. The authors would like to thank Dr. D. Reeves for valuable discussions.

REFERENCES

Coffey W T, Cregg P J, Kalmykov Y P (1993), "On the theory of Debye and Néel relaxation of single domain ferromagnetic particles," in *Advances in Chemical Physics*, Hoboken, NJ, USA: Wiley, vol. 83, doi: 10.1002/9780470141410.ch5.

Coffey W T, Kalmykov Y P (2012), "Thermal fluctuations of magnetic nanoparticles: Fifty years after Brown," *J. Appl. Phys.*, vol. 112, 121301, doi: 10.1063/1.4754272.

Ferguson R M (2011), "Tracer design for magnetic particle imaging: Modeling, synthesis, and experimental optimization of biocompatible iron oxide nanoparticles," Ph.D. dissertation, Univ. Washington, Seattle, WA, USA.

Gleich B, Weizenecker J (2005), "Tomographic imaging using the nonlinear response of magnetic particles," *Nature*, vol. 435, pp. 1214–1217, doi: 10.1038/nature03808.

Hensley D, Goodwill P, Croft L, Conolly S (2015), "Preliminary experimental X-space color MPI," in *Proc. 5th Int. Workshop Magn. Particle Imaging (IWMPI)*, doi: 10.1109/IWMPI.2015.7106993.

Hufschmid R, Arami H, Ferguson R M, Gonzales M, Teeman E, Brush L N, Browning N D, Krishnan K M (2015), "Synthesis of phase-pure and monodisperse iron oxide nanoparticles by thermal decomposition," *Nanoscale*, vol. 7, pp. 11142–11154, doi: 10.1039/c5nr01651g.

Kemp S J, Ferguson R M, Khandhar A P, Krishnan K M (2016), "Monodisperse magnetite nanoparticles with nearly ideal saturation magnetization," *RSC Adv.*, vol. 6, pp. 77452–77464, doi: 10.1039/C6RA12072E.

Kloeden P E, Platen E (1992), "Higher-order implicit strong numerical schemes for stochastic differential equations," *J. Stat. Phys.*, vol. 66, pp. 283–314, doi: 10.1007/BF01060070.

Krishnan K M (2010), "Biomedical nanomagnetics: A spin through possibilities in imaging, diagnostics, and therapy," *IEEE Trans. Magn.*, vol. 46, no. 7, pp. 2523–2558, doi: 10.1109/TMAG.2010.2046907.

Krishnan K M (2016), *Fundamentals and Applications of Magnetic Materials*. London, U.K.: Oxford Univ. Press, pp. 595–600.

Lee D H, Jung J M, Kim S Y, Kim K T, Cho Y I (2012), "Comparison tests for plasma viscosity measurements," *Int. Commun. Heat Mass Transf.*, vol. 39, pp. 1474–1477, doi: 10.1016/j.icheatmasstransfer.2012.10.018.

Ludwig F, Remmer H, Kuhlmann C, Wawrzik T, Arami H, Ferguson R M, Krishnan K M (2014), "Self-consistent magnetic properties of magnetite tracers optimized for magnetic particle imaging measured by ac susceptometry, magnetorelaxometry and magnetic particle spectroscopy," *J. Magn. Magn. Mater.*, vol. 360, pp. 169–173, doi: 10.1016/j.jmmm.2014.02.020.

Rahmer J, Halkola A, Gleich B, Schmale I, Borgert J (2015), "First experimental evidence of the feasibility of multi-color magnetic particle imaging," *Phys. Med. Biol.*, vol. 60, pp. 1775–1791, doi: 10.1088/0031-9155/60/5/1775.

Rauwerdink A M, Giustini A J, Weaver J B (2010), "Simultaneous quantification of multiple magnetic nanoparticles," *Nanotechnology*, vol. 21, 455101, doi: 10.1088/0957-4484/21/45/455101.

Rauwerdink A M, Weaver J B (2011), "Concurrent quantification of multiple nanoparticle bound states," *Med. Phys.*, vol. 38, pp. 1136–1140, doi: 10.1118/1.3549762.

Reeves D B, Weaver J B (2015), "Combined Néel and Brown rotational Langevin dynamics in magnetic particle imaging, sensing, and therapy," *Appl. Phys. Lett.*, vol. 107, 223106, doi: 10.1063/1.4936930.

Rosensweig R E (2002), "Heating magnetic fluid with alternating magnetic field," *J. Magn. Magn. Mater.*, vol. 252, pp. 370–374, doi: 10.1016/S0304-8853(02)00706-0.

Shah S A, Ferguson R M, Krishnan K M (2014), "Slew-rate dependence of tracer magnetization response in magnetic particle imaging," *J. Appl. Phys.*, vol. 116, 163910, doi: 10.1063/1.4900605.

Shah S A, Reeves D M, Ferguson R M, Weaver J B, Krishnan K M (2015), "Mixed Brownian alignment and Néel rotations in superparamagnetic iron oxide nanoparticle suspensions driven by an ac field," *Phys. Rev. B*, vol. 92, 094438, doi: 10.1103/PhysRevB.92.094438.

Weaver J B, Rauwerdink A M, Sullivan C R, Baker I (2008), "Frequency distribution of the nanoparticle magnetization in the presence of a static as well as a harmonic magnetic field," *Med. Phys.*, vol. 35, pp. 1988–1994, doi: 10.1118/1.2903449.

Weizenecker J, Gleich B, Rahmer J, Dahnke H, Borgert J (2009), "Three-dimensional real-time *in vivo* magnetic particle imaging," *Phys. Med. Biol.*, vol. 54, pp. L1–L10, doi: 10.1088/0031-9155/54/5/L01.

Wu K, Wang Y, Feng Y, Yu L, Wang J-P (2015), "Colorize magnetic nanoparticles using a search coil based testing method," *J. Magn. Magn. Mater.*, vol. 380, pp. 251–254, doi: 10.1016/j.jmmm.2014.10.034.